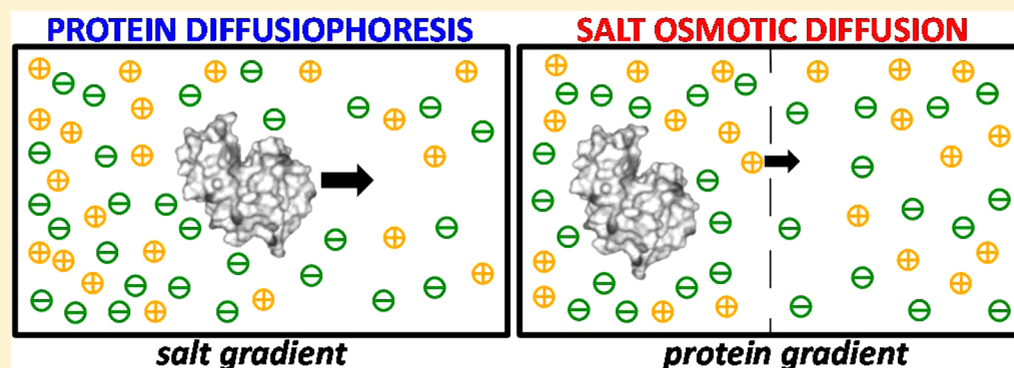


Protein Diffusiophoresis and Salt Osmotic Diffusion in Aqueous Solutions

Onofrio Annunziata,* Daniela Buzatu,[†] and John G. Albright

Department of Chemistry, Texas Christian University, Fort Worth, Texas 76129, United States

 Supporting Information

ABSTRACT: Diffusion of a solute can be induced by the concentration gradient of another solute in solution. This transport mechanism is known as cross-diffusion. We have investigated cross-diffusion in a ternary protein–salt–water system. Specifically, we measured the two cross-diffusion coefficients for the lysozyme–NaCl–water system at 25 °C and pH 4.5 as a function of protein and salt concentrations by Rayleigh interferometry. One cross-diffusion coefficient characterizes salt osmotic diffusion induced by a protein concentration gradient, and is related to protein–salt thermodynamic interactions as described by the theories of Donnan membrane equilibrium and protein preferential hydration. The other cross-diffusion coefficient characterizes protein diffusiophoresis induced by a salt concentration gradient, and is described as the difference between a preferential-interaction coefficient and a transport parameter. We first relate our experimental results to the protein net charge and the thermodynamic excess of water near the protein surface. We then extract the Stefan–Maxwell diffusion coefficient describing protein–salt interactions in water. We find that the value of this coefficient is negative, contrary to the friction interpretation of Stefan–Maxwell equations. This result is explained by considering protein hydration. Finally, protein diffusiophoresis is quantitatively examined by considering electrophoretic and hydration effects on protein migration and utilized to accurately estimate lysozyme electrophoretic mobility. To our knowledge, this is the first time that protein diffusiophoresis has been experimentally characterized and a protein–salt Stefan–Maxwell diffusion coefficient reported. This work represents a significant contribution for understanding and modeling the effect of concentration gradients in protein–salt aqueous systems relevant to diffusion-based mass-transfer technologies and transport in living systems.

INTRODUCTION

Diffusion in liquids^{1–4} is important for applications in which concentration gradients occur such as controlled-release technologies,^{5,6} separation science,⁷ phase transitions,^{8,9} dynamics of living systems,^{10–12} reaction kinetics including pattern formation,^{13–15} and fluid dynamics^{16,17} in general. Diffusion is especially important for mass-transfer applications in which convection is eliminated, for example, by using capillaries or porous media.^{9,18} This transport process plays also an important role in microfluidic technologies.^{19–23}

One not-well-understood aspect of diffusion in multi-component systems is the mechanism of cross-diffusion;^{1,24–29} i.e., diffusion of a solute can be induced by the concentration gradient of another solute in solution. Cross-diffusion is expected to significantly contribute to the drying processes involving polymer–solvent mixtures,³⁰ transport across semi-

permeable membranes⁷ for dialysis applications, and the mechanism of pattern formation in reaction–diffusion systems.²⁸ Another phenomenon that can be linked to cross-diffusion is diffusiophoresis.^{31–33} This can be described as the migration of one colloidal particle induced by the concentration gradient of low-molecular-weight solutes. Interestingly, salt-induced diffusiophoresis has been observed inside microfluidic devices.^{20,34} Thus, it is believed that salt concentration gradients with tunable amplitude and direction could be used to achieve a strongly amplified particle migration inducing either spreading or focusing of the particles in solution.

Received: August 1, 2012

Revised: September 24, 2012

Published: September 26, 2012

Cross-diffusion effects are often modeled by employing the Stefan–Maxwell (S–M) equations.^{35,36} Here, the concentration gradients are replaced by the chemical-potential gradients, the actual driving forces for diffusion. Specifically, the chemical-potential gradients of all diffusing species are written as linear combinations of differences in diffusion rates between two species. The coefficients of these linear combinations consist of a symmetric matrix of friction coefficients describing two-species interactions. The S–M diffusion coefficients are defined as inversely proportional to the individual friction coefficients. It is important to observe that, while the S–M diffusion coefficients associated with the solvent–solute interactions are normally known, those describing the interaction between two solute species are typically unknown and are often estimated from empirical equations.^{29,36}

Due to the applications mentioned above, cross-diffusion studies are expected to be very important for protein aqueous solutions. Indeed, protein systems usually contain other low-molecular-weight solutes. These are necessary for tuning electrostatic interactions (salts),³⁷ stabilizing/destabilizing the protein native state,³⁸ modulating enzymatic activity,^{39,40} mimicking physiological conditions, and promoting protein crystallization.⁴¹

Most protein diffusion studies have been performed using dynamic light scattering (DLS).^{42–44} In multicomponent systems, the measured diffusion coefficient approximately^{45,46} characterizes protein diffusion due to its own concentration gradient. By applying the theory of Brownian motion,⁴⁷ this coefficient has been primarily used to calculate the hydrodynamic radius of the investigated macromolecules;^{48,49} however, DLS cannot be used to characterize cross-diffusion.^{45,46}

Experimental and theoretical diffusiophoresis studies have been performed on large (size of the order of 100 nm) colloid particles.^{33,34} Theoretical studies have focused on understanding how the concentration gradients of low-molecular-weight solutes produce local pressure gradients at the interface between a rigid particle and the surrounding fluid. The resulting force causes particle migration. However, the extrapolation of these studies to the relatively smaller proteins (size range 1–10 nm) may be questionable. For example, the effects of protein preferential solvation are expected to be very important for protein diffusiophoresis. Moreover, diffusiophoresis does not address the other cross-diffusion mechanism, i.e., diffusion of the low-molecular-weight solute induced by the concentration gradient of large particles. Here, we will denote this other cross-diffusion mechanism as “osmotic diffusion” due to its strong ties to thermodynamic interactions. This term was first introduced by Toor in 1957 for multicomponent gas mixtures.⁵⁰

Few experimental cross-diffusion studies on protein–salt aqueous solutions have been performed at 25 °C. Cross-diffusion was investigated in the case of bovine serum albumin using a conductometric method.²⁶ However, these studies were limited to low salt concentrations. The remaining experimental studies were performed at this laboratory on lysozyme as a function of salt concentration at one protein concentration using the Rayleigh interferometric method.^{25,51–54} The high precision of the experimental results and the wide range of salt concentrations have been crucial for characterizing the relation of protein–salt thermodynamic interactions to salt osmotic diffusion.^{51–55} Indeed, salt osmotic diffusion could be linked to the preferential-interaction theory developed by Timasheff and

Record.^{56,57} However, in relation to protein diffusiophoresis, the proposed theoretical models did not describe the corresponding experimental results satisfactorily. Moreover, since these studies were performed at one protein concentration only, it was unclear whether the effect of protein–protein net interactions on protein cross-diffusion could be neglected. This aspect is crucial since a diffusiophoresis model would describe protein cross-diffusion in the limit of zero protein concentration.

In this paper, we report measurements of cross-diffusion coefficients for lysozyme as a function of protein concentration at four NaCl concentrations, pH 4.5, and 25 °C. Our experimental results have allowed us to characterize protein diffusiophoresis and salt osmotic diffusion as a function of salt concentration in the limit of zero protein concentration. We propose a new model on protein diffusiophoresis, which is based on protein charge and hydration effects. Our experimental results were also utilized to estimate the electrophoretic mobility of lysozyme and determine the S–M diffusion coefficient characterizing the solute–solute interaction between protein and salt ions. This work represents a major addition to our previous reports on lysozyme–salt–water systems.^{25,51–55,58}

Fick’s First Law. Cross-diffusion coefficients are defined by the extended Fick’s first law,^{24–26} which describes the diffusion fluxes of the solute components as a linear combination of the corresponding solute concentration gradients. For our ternary protein (1)–salt (2)–water (0) system, we have²⁵

$$-J_1 = D_{11}\nabla C_1 + D_{12}\nabla C_2 \quad (1a)$$

$$-J_2 = D_{21}\nabla C_1 + D_{22}\nabla C_2 \quad (1b)$$

Here, C_i is the molar concentration of solute i (with $i = 1, 2$), J_i is its corresponding flux, and the four D_{ij} ’s (with $i, j = 1, 2$) are the diffusion coefficients. The main-diffusion coefficients, D_{11} and D_{22} , describe the flux of a solute component (protein (1) or salt (2)) due to its own concentration gradient, while the cross-diffusion coefficients, D_{12} and D_{21} , describe the flux of a solute due to the concentration gradient of the other solute. Diffusion coefficients can be reported relative to different reference frames and eqs 1a and 1b are applicable in volume-fixed, solvent-fixed, and other frames. Diffusion coefficients are measured in the laboratory-fixed frame, which is an excellent approximation of the volume-fixed frame.^{59–61}

Normalized Cross-Diffusion Coefficients. The goal of this section is to introduce two normalized cross-diffusion coefficients, \hat{D}_{12} and \hat{D}_{21} , which will be utilized to characterize the behavior of protein diffusiophoresis and salt osmotic diffusion respectively as a function of salt concentration in the limit of zero protein concentration. These coefficients will be directly calculated from the measured cross-diffusion coefficients, D_{12} and D_{21} , and known properties such as the protein tracer-diffusion coefficient and the thermodynamic and transport properties of the binary salt–water system.

To introduce the definitions of \hat{D}_{12} and \hat{D}_{21} , we start from the linear laws of irreversible thermodynamics. These laws are simpler in the solvent-fixed frame than in the volume-fixed frame. Thus, our measured volume-fixed diffusion coefficients were converted into the corresponding solvent-fixed coefficients by utilizing well-established equations based on the partial molar volumes, \bar{V}_i , obtained from density measurements (see the Supporting Information).^{59,62}

Linear laws of irreversible thermodynamics for isothermal diffusion describe diffusion in terms of gradients of solute chemical potentials, μ_i .⁶¹ For our ternary system, we have⁵³

$$-J_1 = L_{11}\nabla\mu_1 + L_{12}\nabla\mu_2 \quad (2a)$$

$$-J_2 = L_{21}\nabla\mu_1 + L_{22}\nabla\mu_2 \quad (2b)$$

where L_{ij} are the Onsager transport coefficients in the solvent-fixed frame. The L_{ij} matrix is symmetric, and $L_{12} = L_{21}$ represents the Onsager reciprocal relation.^{63,64} We can use eqs 1a, 1b, 2a, and 2b to relate the solvent-fixed diffusion coefficients to the L_{ij} according to

$$D_{11} = L_{11}\mu_{11} + L_{12}\mu_{21} \quad (3a)$$

$$D_{12} = L_{11}\mu_{12} + L_{12}\mu_{22} \quad (3b)$$

$$D_{21} = L_{21}\mu_{11} + L_{22}\mu_{21} \quad (3c)$$

$$D_{22} = L_{21}\mu_{12} + L_{22}\mu_{22} \quad (3d)$$

where $\mu_{ij} \equiv (\partial\mu_i/\partial C_j)_{T,p,C_k,k\neq j}$ are the molarity-based chemical-potential derivatives, T is the absolute temperature, and p is the pressure.

Equations 3a–3d provide the means to introduce the two normalized cross-diffusion coefficients, \hat{D}_{12} and \hat{D}_{21} . If we divide D_{12} and D_{21} by $L_{11}\mu_{22}$ and $L_{22}\mu_{22}$, respectively, eqs 3b and 3c become

$$\frac{D_{12}}{L_{11}\mu_{22}} = \frac{\mu_{12}}{\mu_{22}} + \frac{L_{12}}{L_{11}} \quad (4a)$$

$$\frac{D_{21}}{L_{22}\mu_{22}} = \frac{\mu_{21}}{\mu_{22}} + \frac{\mu_{11}L_{11}}{\mu_{22}L_{22}} \frac{L_{12}}{L_{11}} \quad (4b)$$

In the limit of $C_1 \rightarrow 0$, $\mu_{11}/RT = 1/C_1$ and the protein main-diffusion coefficient, $D_{11} = L_{11}\mu_{11}$, becomes the corresponding tracer-diffusion coefficient, D_p , characterizing protein Brownian mobility in solution. Correspondingly, $D_{22} = L_{22}\mu_{22}$ becomes D_s , the solvent-fixed salt diffusion coefficient in the binary salt–water system. Moreover, we can write $\mu_{22}/RT = 2y_s/C_2$ with $y_s = 1 + d \ln y_{\pm}/d \ln C_2$ being the binary salt–water thermodynamic factor and y_{\pm} its mean ionic activity coefficient. The factor “2” in the expression of μ_{22}/RT applies to NaCl and symmetric electrolytes in general. It follows that $L_{11}\mu_{11}$, $L_{11}\mu_{22}$ and $L_{22}\mu_{22}$ in eqs 4a and 4b can be rewritten in the following way:

$$L_{11}\mu_{11} = D_p \quad (5a)$$

$$L_{11}\mu_{22} = C_1(2y_s/C_2)D_p \quad (5b)$$

$$L_{22}\mu_{22} = D_s \quad (5c)$$

Note that D_p , D_s , and y_s are functions of the salt concentration. The values of D_s and y_s are available through the literature of electrolyte solutions. The value of D_p , in our case, will be obtained by extrapolating the ternary protein diffusion coefficient, D_{11} , to $C_1 = 0$. Extrapolation of DLS protein-diffusion coefficients to $C_1 = 0$ can be also employed to determine $D_p(C_2)$.^{42–45}

On the basis of eqs 4a, 4b, 5b, and 5c, we define two normalized limiting cross-diffusion coefficients as

$$\hat{D}_{12} \equiv \lim_{C_1 \rightarrow 0} [C_2 D_{12} / (2y_s C_1 D_p)]$$

for protein diffusiophoresis

$$\hat{D}_{21} \equiv \lim_{C_1 \rightarrow 0} (D_{21}/D_s) \quad \text{for salt osmotic diffusion}$$

Note that \hat{D}_{12} is the ratio between the diffusiophoresis mobility^{31–33} of a particle and its Brownian mobility. The factor $2y_s$ takes into account electrolyte dissociation properties and thermodynamic nonideality.⁶⁵ On the other hand, as will be described below, \hat{D}_{21} is approximately a salt partitioning coefficient.

The thermodynamic quotients μ_{12}/μ_{22} and μ_{21}/μ_{22} are mathematically linked to each other.^{61,62} In the limit of $C_1 \rightarrow 0$, we have

$$\frac{\mu_{12}}{\mu_{22}} = \gamma + \frac{C_2 \bar{V}_2}{2y_s(1 - C_2 \bar{V}_2)} \cong \gamma \quad (6a)$$

$$\frac{\mu_{21}}{\mu_{22}} = -(1 - C_2 \bar{V}_2)\gamma + C_2 \bar{V}_1 \cong \gamma + C_2 \bar{V}_1 \quad (6b)$$

where we have introduced $\gamma \equiv -\lim_{C_1 \rightarrow 0} (\partial m_2 / \partial m_1)_{\mu_2, T, p}$ with m_i being the molality of component i . Note that γ is defined as the negative of the protein–salt preferential-interaction coefficient.^{56,57,66} Preferential-interaction coefficients have been measured for several protein systems using equilibrium dialysis and vapor pressure osmometry.^{56,67} Since these are negative for proteins in the presence of salting-out agents such as NaCl for lysozyme, we have introduced $\gamma > 0$ for convenience. The term $C_2 \bar{V}_2 (2y_s)^{-1} (1 - C_2 \bar{V}_2)^{-1}$ in eq 6a is very small (0.0025 and 0.0092 at $C_2 = 0.25$ and 0.90 mol dm⁻³, respectively) compared to γ (as will be appreciated later) and can be neglected. Similarly, we will also neglect $(1 - C_2 \bar{V}_2)$ in eq 6b since the error associated with the approximation $(1 - C_2 \bar{V}_2)\gamma \cong \gamma$ is 1.7% at the highest experimental salt concentration.

If we now insert eqs 5a, 6a, and 6b into eqs 4a and 4b, protein diffusiophoresis and salt osmotic diffusion are respectively described by

$$\hat{D}_{12} = \gamma - \lambda \quad (7a)$$

$$\hat{D}_{21} = \gamma + \bar{V}_1 C_2 - \alpha \lambda \quad (7b)$$

where $\alpha \equiv D_p/D_s$ and we introduce $\lambda \equiv -\lim_{C_1 \rightarrow 0} (L_{12}/L_{11})$ as a fundamental transport parameter describing protein–salt interaction. An expression for λ will be derived from the S–M equations later (see Discussion).

As shown by eq 7a, protein diffusiophoresis equally depends on both the thermodynamic and transport parameters. On the other hand, because D_p is small compared to D_s (see Results), the value of $\alpha\lambda$ contributes only about 10% to \hat{D}_{21} in eq 7b. Thus, $\hat{D}_{21}(C_2)$ is approximately a thermodynamic quantity related to $\gamma(C_2)$. That \hat{D}_{21} is approximately a thermodynamic quantity can be understood by considering eq 1b. If protein diffusion in the presence of its own concentration gradient is significantly slow, the relatively fast salt diffusion will lead to a quasi-equilibrium condition, $J_2 = 0$, in the presence of a much slower dispersing protein concentration gradient. This leads to $D_{21}/D_{22} \approx -(\partial C_2 / \partial C_1)_{\mu_2, T, p}$ where salt osmotic diffusion due to the protein concentration gradient is counterbalanced by salt diffusion due to its own concentration gradient.⁵⁴ Note that this

setting is analogous to that of salt partitioning across a membrane not permeable to protein macromolecules. In other words, the quotient \hat{D}_{21} approximately describes the difference in salt concentration between two solutions of different protein concentrations at equilibrium. We note that our description of \hat{D}_{21} resembles that of the reaction equilibrium constant being the ratio of the kinetic constants of forward and reverse reaction steps.

In the Results, the measured $D_{ij}(C_1, C_2)$ will be utilized to first extract $\hat{D}_{12}(C_2)$ and $\hat{D}_{21}(C_2)$ and then calculate $\gamma(C_2)$ and $\lambda(C_2)$ from eqs 7a and 7b. All these quantities will be then theoretically examined in the Discussion.

EXPERIMENTAL SECTION

Materials. Six times recrystallized and lyophilized egg-white lysozyme was purchased from Seikagaku America and used without further purification. Deionized water was distilled and then passed through a four-stage Millipore filter system to provide high-purity water for all the experiments.²⁵ A protein–water stock solution was prepared by weight. The molecular weight of lysozyme was taken to be 14 307 g mol⁻¹. Corrections were made for the chloride ion weight fraction in the lysozyme samples as shown in ref 25. Mallinckrodt 99.9% analytical reagent grade NaCl was dried at 400 °C overnight and used without further purification.

Solution Preparation. Precise masses of lysozyme stock solutions and dried NaCl were added to flasks and diluted with pure water. Dilute HCl was added to adjust the pH to 4.5. Any residual solution on the pH electrode was washed back into the solutions, and the dilutions were completed by mass to reach the final target lysozyme and NaCl concentrations. A Corning 135 pH meter with an Orion 8102 ROSS combination pH electrode, standardized with Corning reference solutions, was used to measure the pH of the solutions used for diffusion measurements. It is important to observe that adjusting the solution pH becomes more difficult as the lysozyme concentration decreases, especially for those solutions with lysozyme concentrations lower than 0.3 mM. This can be related to the correspondingly reduced self-buffering properties of lysozyme. The densities of these solutions were measured to determine the corresponding molar concentrations and to calculate partial molar volumes.⁶⁸ All density measurements were made using a computer-interfaced Mettler-Paar DMA40 density meter, thermostatted with water from a large, well-regulated (± 0.01 °C) water bath.

Rayleigh Interferometry. Ternary mutual diffusion coefficients were measured at 25.00 °C with a Gosting diffusometer operating in the Rayleigh interferometric optical mode.^{25,69} The refractive-index profile inside a diffusion cell is measured as described in ref 25 and references therein. Fifty refractive-index profiles were obtained during the course of each experiment. Experiments were performed by the free-diffusion method in a 10 cm vertical diffusion cell with a 2.5 cm horizontal optical path length and a 0.3 cm width. The temperature was regulated to ± 0.001 °C precision and ± 0.01 °C accuracy. Initial step-function distributions of solute concentrations were prepared using a pair of bottom and top uniform solutions with the boundary located at the center of the cell. All experimental data were obtained before detectable concentration changes occurred at the top and bottom ends of the cell, consistent with the free-diffusion boundary condition.

The pair of bottom and top solutions must have different compositions in order to generate a concentration gradient

during each diffusion experiment. For each pair of solutions, we report the mean molar concentrations of lysozyme (1) and NaCl (2) (C_1, C_2). A minimum of two experiments is required for determining the four ternary diffusion coefficients. These two experiments must have different combinations of solute concentration differences across the diffusion boundary. The two chosen experiments are those in which either the salt or the protein concentration of the two solutions is different while the corresponding concentration of the other solute is the same. To verify reproducibility, two other duplicate experiments were performed at each set of mean concentrations. The volume-fixed diffusion coefficients were obtained by applying the method of nonlinear least squares to the extracted profiles of the refractive index.⁷⁰ The corresponding solvent-fixed values were then calculated (see the Supporting Information).^{59,62} Values are reported in Table 1. Note that the experiment with

Table 1. Ternary Diffusion Coefficients in Solvent-Fixed Frame for the Lysozyme–NaCl–Water System at 25 °C and pH 4.5

$C_1/10^{-3}$ mol dm ⁻³	C_2/mol dm ⁻³	$D_{11}/10^{-9}$ m ² s ⁻¹	$D_{12}/10^{-9}$ m ² s ⁻¹	$D_{21}/10^{-9}$ m ² s ⁻¹	$D_{22}/10^{-9}$ m ² s ⁻¹
0.300	0.250	0.1276	0.000 095	9.5	1.473
0.450	0.250	0.1271	0.000 139	9.2	1.468
0.600	0.250	0.1263	0.000 186	10.3	1.466
0.700	0.250	0.1261	0.000 207	9.9	1.462
1.000	0.250	0.1251	0.000 299	9.1	1.453
1.500	0.250	0.1232	0.000 432	8.9	1.437
2.500	0.250	0.1196	0.000 688	8.9	1.401
0.300	0.500	0.1225	0.000 064	13.7	1.477
0.450	0.500	0.1211	0.000 093	14.5	1.471
0.600	0.500	0.1191	0.000 124	14.5	1.469
1.000	0.500	0.1154	0.000 200	14.1	1.456
1.500	0.500	0.1105	0.000 293	13.9	1.440
2.500	0.500	0.1018	0.000 468	13.4	1.407
0.300	0.650	0.1199	0.000 059	18.7	1.482
0.450	0.650	0.1181	0.000 084	17.9	1.478
0.600	0.650	0.1156	0.000 112	17.0	1.474
0.800	0.650	0.1138	0.000 150	16.6	1.467
1.000	0.650	0.1114	0.000 185	16.1	1.462
1.200	0.650	0.1090	0.000 222	16.1	1.455
1.500	0.650	0.1058	0.000 276	17.3	1.444
0.300	0.900	0.1163	0.000 050	20.9	1.499
0.450	0.900	0.1138	0.000 079	20.6	1.489
0.600	0.900	0.1111	0.000 104	21.2	1.488
1.000	0.900	0.1054	0.000 169	21.7	1.473

the initial protein concentration gradient dominates the determination of D_{21} while that with the initial salt concentration gradient dominates the determination of D_{12} .

We find that the values of D_{21} at lysozyme concentrations lower than 0.60 mM somewhat deviate from the observed behavior at higher protein concentrations when plotting this coefficient as a function of C_1 . These deviations did not correlate with salt concentration. To a smaller extent, this behavior was also observed for D_{12} when plotting D_{12}/C_1 as a function of C_1 . These observed deviations can be attributed to the important role of the protein charge on the value of the cross-diffusion coefficients (as shown by eqs 12 and 24) and the difficulties of adjusting the solution pH when the protein concentration is too low. Indeed, the experiments with the initial protein concentration gradient require a relatively low

protein concentration in one of the two prepared solutions. Hence, we will consider $D_{12}(C_1, C_2)$ and $D_{21}(C_1, C_2)$ only for the experimental data at lysozyme concentrations of 0.60 mM and higher. Nonetheless, it is important to remark that the inclusion of the cross-diffusion data at low protein concentrations in our analysis does not produce appreciably different results.

RESULTS

All our experimental results on the four ternary diffusion coefficients in the solvent-fixed frame are reported in Table 1. Note that the two main-diffusion coefficients (in the volume-fixed frame) were discussed in our previous papers.^{45,58} The determination of \hat{D}_{12} from D_{12} requires y_s and D_p data. On the other hand, \hat{D}_{21} can be determined by the direct extrapolation of D_{21}/D_{22} data to $C_1 = 0$. In Table 2, we report the salt–water

Table 2. Transport and Thermodynamic Parameters

$C_2/\text{mol dm}^{-3}$	y_s	$D_p/10^{-9} \text{ m}^2 \text{ s}^{-1}$	α
0.250	0.915	$0.1287 \pm 0.0001^{a,b}$	0.0866
0.500	0.930	0.1258 ± 0.0002^c	0.0840
0.650	0.943	0.1239 ± 0.0005^c	0.0824
0.900	0.968	0.1208 ± 0.0004^d	0.0800

^aThe reported errors are standard deviations. ^bValue obtained from linear and quadratic extrapolation. ^cValues obtained from quadratic extrapolation. ^dValue obtained from linear extrapolation.

thermodynamic factor, y_s , as a function of C_2 . These data were obtained by interpolation of available literature data.^{71,72} The values of the lysozyme tracer-diffusion coefficient, D_p , as a function of NaCl concentration are also reported in Table 2. These were determined by extrapolating D_{11} to $C_1 = 0$ at constant C_2 .

According to the Stokes–Einstein equation, the observed decrease of D_p as C_2 increases is related to the corresponding increase in the viscosity of the binary salt–water solution. If we correct for salt viscosity,⁷³ we obtain $D_p = (0.1316 \pm 0.0002) \times 10^{-9} \text{ m}^2 \text{ s}^{-1}$ at $C_2 = 0$. This corresponds to the equivalent hydrodynamic radius of $R_p = 1.864 \text{ nm}$ based on the value of $0.8902 \times 10^{-3} \text{ kg m}^{-1} \text{ s}^{-1}$ for water viscosity.⁷⁴ The values of D_p were also utilized together with the literature values of the salt diffusion coefficient,⁷¹ D_s , to calculate the diffusion ratio α relevant to eq 7b. Our results are also included in Table 2 as a function of C_2 . Since the term in eq 7b containing α is relatively small, we can assume that this parameter is a constant independent of salt concentration. Thus, we set $\alpha = 0.083$ equal to the average of the data reported in Table 2.

Our ternary diffusion data in Table 1 together with the transport and thermodynamic parameters in Table 2 can be used to calculate the quotients $C_2 D_{12}/(2C_1 y_s D_p)$ and D_{21}/D_{22} . In the limit of $C_1 = 0$, these two quantities become \hat{D}_{12} and \hat{D}_{21} , respectively. To determine $\hat{D}_{12}(C_2)$ and $\hat{D}_{21}(C_2)$, we consider the following linear expressions:

$$(C_2 D_{12})/(2y_s C_1 D_p) = (1 - k_{12} C_1) \hat{D}_{12} \quad (8a)$$

$$D_{21}/D_{22} = (1 - k_{21} C_1) \hat{D}_{21} \quad (8b)$$

where k_{12} and k_{21} characterize the first-order effect of protein concentration on the normalized cross-diffusion coefficients. Relative to the experimental error, we will assume that these two parameters are independent of salt concentration. The dependence of \hat{D}_{12} and \hat{D}_{21} on salt concentration can be

described by the following linear functions within our experimental range of salt concentrations:

$$\hat{D}_{12} = a_{12} + b_{12} C_2 \quad (9a)$$

$$\hat{D}_{21} = a_{21} + b_{21} C_2 \quad (9b)$$

Equations 9a and 9b are consistent with the assumption that $\gamma(C_2)$ and $\lambda(C_2)$ are also described by corresponding linear functions. Thus, we can write

$$\gamma = \gamma^0 + \gamma' C_2 \quad (10a)$$

$$\lambda = \lambda^0 + \lambda' C_2 \quad (10b)$$

Note that we have $a_{12} = \gamma^0 - \lambda^0$, $b_{12} = \gamma' - \lambda'$, $a_{21} = \gamma^0 - \alpha \lambda^0$, and $b_{21} = \gamma' + \bar{V}_1 - \alpha \lambda'$ from eqs 7a and 7b. Figures 1 and 2

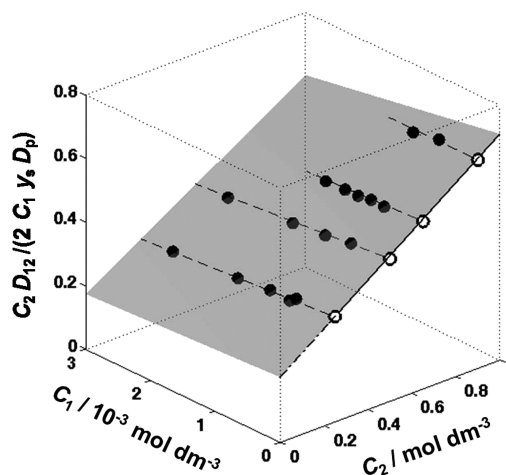


Figure 1. Normalized cross-diffusion coefficient, $C_2 D_{12}/(2C_1 y_s D_p)$, as a function of C_1 and C_2 (solid circles). The gray planar surface describes eqs 8a and 9a with the values of k_{12} , a_{12} , and b_{12} reported in Table 3. The solid line at $C_1 = 0$ describes \hat{D}_{12} as a function of C_2 , and its dashed linear extension indicates the value of a_{12} . The four dashed lines describe independent linear fits at constant C_2 , and the open circles are the corresponding intercepts at $C_1 = 0$.

show the behavior of our normalized cross-diffusion coefficients. This is described quite well by eqs 8a, 8b, 9a, and 9b within the experimental concentration range. Based on these equations, we apply the method of multiple linear least squares to our normalized cross-diffusion coefficients with protein concentrations of 0.60 mM or higher, as indicated in the Experimental Section. The results of our fits are reported in Table 3 together with the calculated values of γ^0 , γ' , λ^0 , and λ' . Addition of our data at the two lower protein concentrations leads to an increase of $\approx 20\%$ in the standard error. However, our fit results remain the same within one standard deviation. From the values in Table 3, we can appreciate that γ and λ have comparable magnitudes. Furthermore, we can calculate that $\alpha \lambda$ is 7–8% of γ and 3–5% of $\gamma + \bar{V}_1 C_2$ in eq 7b. Thus, as previously mentioned, the contribution of λ to the behavior of $\hat{D}_{21}(C_2)$ is marginal.

Interestingly, our extracted values of k_{12} and k_{21} reveal that the quotients $C_2 D_{12}/(2C_1 y_s D_p)$ and D_{21}/D_{22} at $C_1 = 0.60 \text{ mM}$ (8.6 g/L) are just 3 and 1% lower than \hat{D}_{12} and \hat{D}_{21} , respectively. Hence, we note that measurements of cross-diffusion coefficients at this one protein concentration can be directly utilized to calculate \hat{D}_{12} and \hat{D}_{21} within the experimental error. Furthermore, if we consider the highest

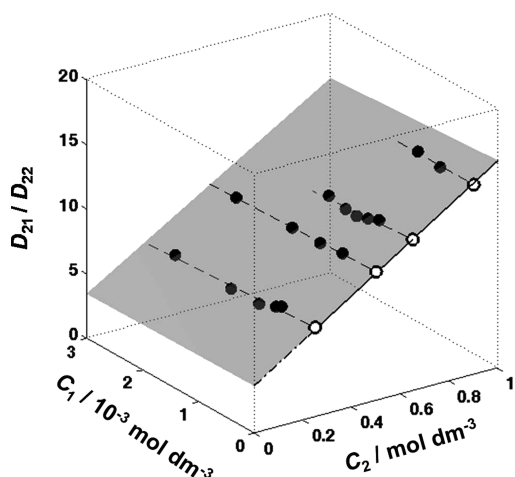


Figure 2. Normalized cross-diffusion coefficient, D_{21}/D_{22} , as a function of C_1 and C_2 (solid circles). The gray planar surface describes eqs 8b and 9b with the values of k_{21} , a_{21} , and b_{21} reported in Table 3. The solid line at $C_1 = 0$ describes \hat{D}_{21} as a function of C_2 , and its dashed linear extension indicates the value of a_{21} . The four dashed lines describe independent linear fits at constant C_2 , and the open circles are the corresponding intercepts at $C_1 = 0$.

Table 3. Fitting Parameters^a

a_{12}	0.203 ± 0.005	a_{21}	3.6 ± 0.3
$b_{12}/\text{mol dm}^{-3}$	0.52 ± 0.01	$b_{21}/\text{mol dm}^{-3}$	12.4 ± 0.4
$k_{12}/10^{-3} \text{ mol dm}^{-3}$	0.050 ± 0.005	$k_{21}/\text{mol dm}^{-3}$	0.020 ± 0.013
λ^0 ^b	3.7 ± 0.4	γ^0 ^d	3.9 ± 0.3
$\lambda'^c/\text{mol dm}^{-3}$	1.8 ± 0.4	$\gamma'^e/\text{mol dm}^{-3}$	2.4 ± 0.4

^aThe reported errors are standard deviations. ^b $\lambda^0 = (a_{21} - a_{12})/(1 - \alpha)$. ^c $\lambda' = (b_{21} - \bar{V}_1 - b_{12})/(1 - \alpha)$. ^d $\gamma^0 = (a_{21} - \alpha a_{12})/(1 - \alpha)$. ^e $\gamma' = (b_{21} - \bar{V}_1 - \alpha b_{12})/(1 - \alpha)$.

experimental concentration of $C_1 = 2.5$ mM (36 g/L), the corresponding two quotients become 13 and 5% lower than \hat{D}_{12} and \hat{D}_{21} , respectively. Thus, the limiting values of \hat{D}_{12} and \hat{D}_{21} can be employed to estimate cross-diffusion coefficients for a broad range of protein concentrations. Indeed, neglecting the effect of C_1 leads to an error of the order of 10%. On the other hand, it is important to remark that \hat{D}_{12} and \hat{D}_{21} strongly depend on salt concentration. Their behavior will be examined in the Discussion.

DISCUSSION

This section is organized in three parts. In the first part, we discuss salt osmotic diffusion as the consequence of protein–salt thermodynamic interactions. It is important to mention that the quotient D_{21}/D_{22} has been previously discussed.^{51–55} In this paper, our refined examination of salt osmotic diffusion will provide the starting point for examining protein diffusiophoresis. In the second part, Stefan–Maxwell Equations, we examine the behavior of the transport parameter, $\lambda(C_2)$. Here, we will introduce the Stefan–Maxwell (S–M) equations for the protein–salt–water system and characterize the protein–salt S–M diffusion coefficient from our experimental results. In the third part, Protein Diffusiophoresis, we will examine the observed protein diffusiophoresis and relate its behavior to protein charge, protein electrophoretic mobility, and protein hydration.

Salt Osmotic Diffusion. As shown in Figure 3, \hat{D}_{21} can be described as a linear function of C_2 with positive slope and

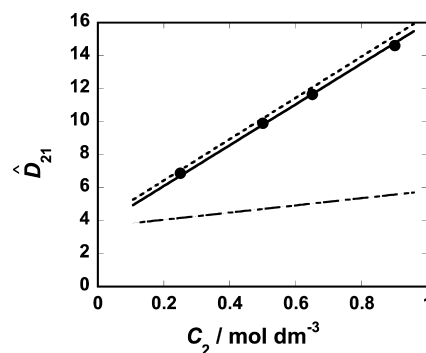


Figure 3. Normalized osmotic-diffusion coefficient, \hat{D}_{21} , as a function of C_2 (solid circles). The solid curve describes the fit of the experimental results. The calculated plot of $\hat{D}_{21}(C_2)$ described by the approximated eq 12 (---) and that of $\gamma(C_2)$ (–) are also shown.

intercept. The observed behavior of $\hat{D}_{21}(C_2)$ can be examined by considering the corresponding behavior of $\gamma(C_2)$. One contribution to the value of $\gamma \cong \mu_{12}/\mu_{22}$ is related to the common-ion effect.^{52,53} The chemical potential of one ionic solute increases as the concentration of the other ionic solute increases due to the corresponding increase in the concentration of the common ion (Cl^- in our case). In the case of proteins, this phenomenon is often illustrated by considering the so-called Donnan equilibrium experiment. Here, we consider the partitioning of salt ions (and water) occurring between a binary salt–water solution and a ternary protein–salt–water solution separated by a membrane not permeable to the protein macro-ions. At equilibrium, the concentration of the salt component will be higher in the binary solution due to the common-ion effect. If the protein has a charge Z_p , the common-ion effect leads to $\gamma = |Z_p|/2$ in the case of a 1:1 electrolyte such as NaCl.⁵⁷

The common-ion effect is expected to dominate at low salt concentration. As the salt concentration increases, protein–salt specific interactions become more important. From a phenomenological point of view, the resulting effect on $\gamma(C_2)$ can be examined by introducing a simple model based on the assumption that a protein macromolecule with the surrounding salt solution can be divided into two domains.^{57,75} The first domain is represented by a macromolecule and its local salt–water layer. This local domain is in chemical equilibrium with the bulk surrounding domain, representing the salt–water remaining solution. Since macromolecules interact with salt ions and water molecules in their vicinity, the salt concentration in the local domain is different from that of the unperturbed bulk domain. If the salt concentration in the local domain is lower than that of the bulk domain, preferential hydration of the protein occurs. If we apply this two-domain model to a neutral macromolecule, we can derive^{54,57,75} that $\gamma = N_w(C_2/C_0)$, where N_w is the excess number of water molecules in the local domain compared to the bulk domain.

For a charged protein, we can add⁶⁴ the common-ion contribution to that of preferential hydration and write

$$\gamma = \frac{|Z_p|}{2} + N_w \bar{V}_0 \frac{C_2}{1 - C_2 \bar{V}_2} \cong \frac{|Z_p|}{2} + N_w \bar{V}_0 C_2 \quad (11)$$

where we have used $C_0 \bar{V}_0 = 1 - C_2 \bar{V}_2$, and $\bar{V}_0 = 0.0181 \text{ dm}^3 \text{ mol}^{-1}$ (see the Supporting Information) is the partial molar volume of water. The values of the intercept, γ^0 , and slope, γ' , reported in Table 3 can be used to determine Z_p and N_w in eq

11, assuming that these parameters are constant. We obtain $Z_p = 7.8 \pm 0.6$ and $N_w = 130 \pm 20$.

We note that this value of Z_p is lower than the titration value of 11 (at pH 4.5).⁷⁶ This result is consistent with the existence of four anion binding sites as observed by X-ray diffraction.^{77,78} Furthermore, counterion binding is consistent with the presence of a “Stern layer” surrounding the charged macromolecule, in which counterions are tightly bound to the particle surface.⁷⁹ Our analysis does not necessarily assume that the protein charge is a constant independent of salt concentration. It implies that a relatively strong counterion binding occurs at ionic strengths significantly lower than those of our experimental range. The weakening of the protein–counterion electrostatic attraction at high ionic strengths and the saturation of counterion sites should prevent counterion binding at high salt concentrations. If a weak binding still occurs, its contribution is incorporated in the N_w term. This preferential-hydration parameter should not be taken as the number of water molecules bound to one protein molecule but as a more general parameter, the thermodynamic excess of water, describing the net preference of a protein macromolecule for water molecules compared to salt ions. Thus, ion binding has the effect of reducing the net value of N_w .^{56,75}

We now turn our attention back to the behavior of $\hat{D}_{21}(C_2)$. If we neglect the contribution of $\alpha\lambda$ in eq 7b and consider eq 11, we can write

$$\hat{D}_{21} \approx |Z_p|/2 + (\bar{V}_1 + N_w\bar{V}_0)C_2 \quad (12)$$

To appreciate the accuracy of eq 12, Figure 3 shows the behavior of $\hat{D}_{21}(C_2)$ based on eq 7b together with that obtained by neglecting the contribution of $\alpha\lambda$. For completeness, we include the behavior of $\gamma(C_2)$ in Figure 3.

The intercept of \hat{D}_{21} in Figure 3 approximately describes the common-ion effect and the corresponding slope is approximately equal to $\bar{V}_1 + N_w\bar{V}_0$. We now note that $\bar{V}_1 + N_w\bar{V}_0$ is approximately the same as $V_p + N_wV_w$, where V_p and V_w are the molar volumes of protein and surrounding water molecules, respectively.⁸⁰ Thus, the slope of \hat{D}_{21} in eq 12 approximately represents the volume per protein mole excluded to the salt component in solution. This slope describes the previously discussed^{25,53} excluded-volume effect.

Stefan–Maxwell Equations. To examine the behavior of $\lambda(C_2)$, we introduce the frictional formalism based on the S–M equations.^{35,36} These equations have the advantage, compared to Fick’s law, of providing a clearer physical interpretation of multicomponent diffusion processes, provided that all main diffusing species have been identified. For a protein–salt–water system, we consider the three ionic species, protein (p), counterion (–), and co-ion (+), and the neutral solvent species, water (w).

According to the S–M formalism, a diffusion process can be thought to occur in a quasi-stationary regime in which the driving forces equal the opposing frictional force caused by the difference in diffusion velocities between species i and species j (with $i, j = p, +, -, w$, and $i \neq j$).⁸¹ The driving forces for ionic diffusion are the electrochemical-potential gradients of the ionic species, $\nabla\tilde{\mu}_i$ (with $i = p, +, -$). Following the theoretical work of Krishna on multicomponent electrolyte systems,⁸² the S–M relations become in our case

$$-C_T \frac{\nabla\tilde{\mu}_p}{RT} = \frac{C_w}{\mathcal{D}_{pw}} \left(\frac{J_p}{C_p} - \frac{J_w}{C_w} \right) + \frac{C_+}{\mathcal{D}_{+p}} \left(\frac{J_p}{C_p} - \frac{J_+}{C_+} \right) + \frac{C_-}{\mathcal{D}_{-p}} \left(\frac{J_p}{C_p} - \frac{J_-}{C_-} \right) \quad (13a)$$

$$-C_T \frac{\nabla\tilde{\mu}_+}{RT} = \frac{C_w}{\mathcal{D}_{+w}} \left(\frac{J_+}{C_+} - \frac{J_w}{C_w} \right) + \frac{C_-}{\mathcal{D}_{+-}} \left(\frac{J_+}{C_+} - \frac{J_-}{C_-} \right) + \frac{C_p}{\mathcal{D}_{+p}} \left(\frac{J_+}{C_+} - \frac{J_p}{C_p} \right) \quad (13b)$$

$$-C_T \frac{\nabla\tilde{\mu}_-}{RT} = \frac{C_w}{\mathcal{D}_{-w}} \left(\frac{J_-}{C_-} - \frac{J_w}{C_w} \right) + \frac{C_+}{\mathcal{D}_{-+}} \left(\frac{J_-}{C_-} - \frac{J_+}{C_+} \right) + \frac{C_p}{\mathcal{D}_{-p}} \left(\frac{J_-}{C_-} - \frac{J_p}{C_p} \right) \quad (13c)$$

where C_i is the molar concentration of the ionic species i (with $i = p, +, -, w$), $C_T = C_w + C_+ + C_- + C_p$ is the total concentration, and R is the ideal-gas constant. Note that $C_w = C_0$, $C_p = C_1$, $C_+ = C_2$, and $C_- = |Z_p|C_1 + C_2$ is the common-ion concentration. In eqs 13a–13c, the expression $J_i/C_i - J_j/C_j$ represents the difference in diffusion velocities between species i and species j , and $J_w = 0$ if we apply the solvent-fixed frame. The six \mathcal{D}_{ij} ’s (with $i, j = p, +, -, w$, and $i \neq j$) are the S–M diffusion coefficients. The corresponding $(RT/C_T)\mathcal{D}_{ij}^{-1}$ are known as friction coefficients.^{81,82} These coefficients are independent of the employed reference frame, and \mathcal{D}_{ij}^{-1} has a direct physical interpretation in terms of a friction coefficient between the species i and j .⁸³

In the limit of $C_1 = 0$, $(C_T/C_w)\mathcal{D}_{pw}$ becomes $D_p(C_2)$, the tracer-diffusion coefficient of the protein, and $2\gamma_s(C_T/C_w) \cdot (\mathcal{D}_{+w}^{-1} + \mathcal{D}_{-w}^{-1})^{-1}$ becomes $D_s(C_2)$, the solvent-fixed diffusion coefficient for the binary salt–water system. In the limit of both $C_1 = 0$ and $C_2 = 0$, we have $\mathcal{D}_{pw} = D_p$, $\mathcal{D}_{+w} = D_+$, and $\mathcal{D}_{-w} = D_-$, where D_p , D_+ , and D_- are the tracer-diffusion coefficients in water of the protein, co-ion, and counterion species, respectively. We know⁸⁴ that $D_+ = 1.33 \times 10^{-9} \text{ m}^2 \text{ s}^{-1}$ and $D_- = 2.03 \times 10^{-9} \text{ m}^2 \text{ s}^{-1}$ at 25 °C for Na^+ and Cl^- , respectively. At infinite dilution, the S–M relations reduce to the Nernst–Planck equations:^{82,85}

$$-J_p = C_p D_p (\nabla\mu_p + Z_p F \nabla\psi) / RT \quad (14a)$$

$$-J_+ = C_+ D_+ (\nabla\mu_+ + F \nabla\psi) / RT \quad (14b)$$

$$-J_- = C_- D_- (\nabla\mu_- - F \nabla\psi) / RT \quad (14c)$$

where F is the Faraday constant. In eqs 14a–14c, we have reported the explicit expressions of the electrochemical-potential gradients of the ionic species in terms of the corresponding gradients of chemical potentials and electrical potential, ψ .

To obtain an expression for $\lambda(C_2)$, we start by considering the following relations between chemical potentials of solute components and ionic species:

$$\nabla\mu_1 = \nabla\mu_p + |Z_p| \nabla\mu_- \quad (15a)$$

$$\nabla\mu_2 = \nabla\mu_+ + \nabla\mu_- \quad (15b)$$

We first combine eqs 13a–13c according to eqs 15a and 15b and eliminate $\nabla\psi$ in the resulting equations (see the Supporting Information). We then replace the fluxes of the ionic species with those of the solutes by applying the electroneutrality condition:

$$J_- = |Z_p|J_p + J_+ \quad (16)$$

with $J_p = J_1$ and $J_+ = J_2$. In this way, we obtain expressions for $\nabla\mu_1$ and $\nabla\mu_2$ as a function of J_1 and J_2 . These can be then inverted to yield explicit expressions for J_1 and J_2 . Comparison with eqs 2a and 2b allows us to obtain expressions for the L_{ij} (with $i, j = 1, 2$) as a function of the S–M diffusion coefficients (see the Supporting Information). If we then apply the definition of λ , we finally obtain

$$\lambda = |Z_p|\tau_+ - \hat{D}_{12}^{-1}C_2/C_0 \cong |Z_p|\tau_+ - \hat{D}_{12}^{-1}\bar{V}_0C_2 \quad (17)$$

where $\tau_i \equiv D_{iw}/(D_{+w} + D_{-w})$ (with $i = +, -$ and $\tau_+ + \tau_- = 1$) is the transference number of the salt ions,⁷¹ and $\hat{D}_{12} \equiv [(D_{+p}^{-1} + D_{-p}^{-1})/(D_{+w}^{-1} + D_{-w}^{-1})]^{-1}$ is a normalized S–M diffusion coefficient describing the protein–salt interaction. The term $D_{+p}^{-1} + D_{-p}^{-1}$ formally represents the total friction between protein and salt ions.

The transference number, τ_+ , decreases about 3% within our salt concentration range, and can be assumed constant.⁷² If we also assume that \hat{D}_{12} can be regarded as a constant, $\lambda(C_2)$ becomes a linear function of salt concentration consistent with our experimental findings (see Results). We can therefore utilize the values of λ^0 and λ' reported in Table 3 to calculate $|Z_p|$ and \hat{D}_{12} , respectively. If we set the value of τ_+ equal to $D_+/ (D_+ + D_-) = 0.396$,⁸³ we calculate $Z_p = 9.3 \pm 1.0$. This value is somewhat higher than that of 7.8 ± 0.6 obtained from the intercept of $\gamma(C_2)$. Nonetheless, they appear to be still in agreement within the experimental error.

We find that $\hat{D}_{12}^{-1} = -100 \pm 20$ is negative from the value of the slope, λ' . To our knowledge, this is the first time that the value of \hat{D}_{12}^{-1} has been extracted for a protein–salt aqueous system. Note that a negative value of \hat{D}_{12}^{-1} is not consistent with the friction interpretation of S–M diffusion coefficients. To emphasize the relevance of this finding, we consider some current equations used to predict D_{ij} for mass-transfer modeling. The predictive equation proposed by Wesselingh and Krishna is $D_{ij} = (D_{iw}D_{jw})^{1/2}$ (with $i, j = p, +, -$ and $i \neq j$).^{29,86} By setting $D_{pw} = D_p$, $D_{+w} = D_+$, and $D_{-w} = D_-$, we estimate $\hat{D}_{12}^{-1} \approx 3.5$. Another predictive equation, $D_{ij} = D_{w0}D_{w0}/D_w$, has been recently proposed by Liu et al.,²⁹ where $D_w = 2.30 \times 10^{-9} \text{ m}^2 \text{ s}^{-1}$ is the self-diffusion coefficient of water.⁸⁷ In this second case, we estimate $\hat{D}_{12}^{-1} \approx 18$. Both estimates show that the value of \hat{D}_{12}^{-1} is positive. We also note that the estimated magnitudes of this coefficient are significantly smaller than our determined value. We remark that negative frictions were also observed for aqueous poly(ethylene glycol), a neutral hydrophilic polymer, in the presence of a neutral cosolvent.⁶² Thus, we cannot attribute this result to the complexity of electrolyte systems.

The extraction of negative values of \hat{D}_{12}^{-1} can be attributed to the incorrect identification of the diffusing species. We hypothesize protein hydration as the chief mechanism of the observed result and the actual diffusing macromolecule is the hydrated protein. If a macromolecule binds n_w water molecules, $\nabla\tilde{\mu}_p$ in eq 13a should be replaced by $\nabla\tilde{\mu}_p + n_w\nabla\mu_0$, the chemical potential of the hydrated protein, with μ_0 being the chemical potential of the solvent component, and $C_0\nabla\mu_0 =$

$-C_1\nabla\mu_1 - C_2\nabla\mu_2$ (Gibbs–Duhem equation).⁸⁸ Furthermore, the solvent-fixed flux of free water species, J_w , is no longer zero due to the condition $J_0 = J_w + n_wJ_p = 0$. If we consider protein hydration as the only contribution to \hat{D}_{12} , we can obtain $\hat{D}_{12}^{-1} = -n_w$ (see the Supporting Information).⁸⁸ This is qualitatively consistent with our findings and allow us to estimate that $n_w \approx 100$.

The n_w water molecules are tightly bound to protein sites and are not exchangeable with salt ions.⁸⁹ Note that this value of lysozyme hydration is comparable to the excess of water, N_w , extracted from eq 11. Although n_w and N_w should be regarded as independent entities, not directly related, these two quantities bear obvious similarities.⁸⁸ Thus, their similar values corroborate the validity of our hypothesis that protein hydration is the dominant mechanism responsible for the observed value of \hat{D}_{12}^{-1} . We therefore conclude that the effect of molecular hydration should be taken into account when predictive equations for the D_{ij} 's are applied to solvated macromolecules.

Protein Diffusiophoresis. We start by examining the relation of \hat{D}_{12} to the protein charge, Z_p . If we insert eqs 11 and 17 into eq 7a and consider the case of $C_2 = 0$ (with $C_1/C_2 = 0$), we derive

$$\hat{D}_{12}(0) = \frac{|Z_p| D_- - D_+}{2 D_- + D_+} \quad (18)$$

Equation 18, which can be also obtained by applying the so-called Nernst–Hartley equations,^{24,26} shows that protein diffusiophoresis is driven by the difference in ionic mobilities, $D_- - D_+$. If there is a difference in mobility between anion and cation species, a salt concentration gradient generates a corresponding internal gradient of electrical potential. If the anion tends to diffuse faster than the cation ($D_- > D_+$), the protein will diffuse toward lower salt concentration ($\hat{D}_{12} > 0$) to maintain electroneutrality.

If we assume that $\hat{D}_{12}(0) = a_{12}$ (see eq 9a) and use the known value of $(D_- - D_+)/ (D_+ + D_-) = 0.208$,⁸³ we can calculate $Z_p = 1.95 \pm 0.05$ from eq 18. Note that this value of Z_p represents only about 20–25% of the charge values reported above. This large discrepancy can be attributed to \hat{D}_{12} not being a linear function of C_2 at low salt concentrations.

It is interesting to observe that even if we have extracted two similar values of Z_p from the $\gamma(C_2)$ and $\lambda(C_2)$, the corresponding value extracted from $\hat{D}_{12} = \gamma(C_2) - \lambda(C_2)$ is very different. This is related to γ and λ being of comparable magnitude: even minor deviations of $\gamma(C_2)$ and $\lambda(C_2)$ from the proposed linear behavior may significantly amplify when the difference, $\gamma - \lambda$, is considered. This shows that models aimed at deriving separate expressions of γ and λ are likely to yield poor results in predicting \hat{D}_{12} . Indeed, considering models that directly yield an expression for \hat{D}_{12} should represent a better approach.

We start to examine \hat{D}_{12} at low salt concentration by considering the similarities between diffusiophoresis and electrophoresis.^{79,90} Protein electrophoresis is described by considering the relation between the electrical-potential gradient, $\nabla\psi$, and the resulting electrophoretic migration velocity, J_1/C_1 :

$$-J_1/C_1 = u_p\nabla\psi \quad (19)$$

Note that J_1 is defined with respect to the solvent-fixed frame because $\nabla\psi$ does not act on the neutral solvent molecules. The

proportionality constant, u_p , is the protein electrophoretic mobility. An expression for the gradient of electrical potential internally generated by the concentration gradient of ionic species can be obtained by applying eq 16 to the Nernst–Planck eqs 14a–14c. In the limit of $C_2 = 0$ (with $C_1/C_2 = 0$), we have

$$-\frac{F\nabla\psi}{RT} = \frac{D_- - D_+}{D_- + D_+} \frac{\nabla C_2}{C_2} \quad (20)$$

The comparison of eq 18 with eq 20 allows us to appreciate that $2RTD_{12}(0)\nabla \ln C_2$ represents the electrical force, $Z_p F\nabla\psi$, felt by the charged protein molecule and responsible for diffusiophoresis. If we substitute eq 20 into eq 19 and apply the definition of \hat{D}_{12} , eq 18 becomes

$$\hat{D}_{12}(0) = \frac{1}{2} \frac{RT}{F} \frac{|u_p(0)|}{D_p} \frac{D_- - D_+}{D_- + D_+} \quad (21)$$

The dependence of \hat{D}_{12} on salt concentration can be examined by examining the corresponding dependence of u_p .^{33,91,92} According to the theory of electrophoresis, the value of $|u_p|/D_p$ is expected to dramatically drop as the solution ionic strength, I , increases. This is related to the electrical double layer surrounding charged particles in electrolyte solutions. The behavior of u_p depends on the corresponding behavior of the zeta potential, ζ , which is the electrical potential at the shear interface between the diffusing particle and the surrounding fluid. If the particle is treated as a dielectric sphere with homogeneous surface charge, and we locate the shear interface at the hydrodynamic radius of the protein, R_p , we have^{91,92}

$$\frac{RTu_p}{FD_p} = f_{\text{elec}}(\kappa R_p) \frac{R_p}{\lambda_B} \frac{F\zeta}{RT} \quad (22)$$

where $\kappa \equiv (8000\pi N_A \lambda_B I)^{1/2}$ is the Debye constant, N_A is Avogadro's number, and $\lambda_B = 0.7151$ nm is the Bjerrum length for water at 298.15 K.⁹³ Note that κ^{-1} describes the thickness of the double layer, and κR_p represents the relative size of the particle compared κ^{-1} . The function

$$f_{\text{elec}}(x) = 1.5 - e^x [7.5E_7(x) - 3E_5(x)]$$

with $E_n(x) = \int_1^\infty t^{-n} e^{-xt} dt$ was first introduced by Henry.^{92,94} The value of this function varies from $f_{\text{elec}}(0) = 1$ for a sphere at zero ionic strength to $f_{\text{elec}}(\infty) = 1.5$ for a planar surface.

Equation 22 ignores the effects of protein shape and surface charge distribution. These effects have been investigated by Allison and Tran on lysozyme as a function of pH.⁷⁹ In this investigation, the calculated protein electrophoretic mobility at $I = 0.15$ M was found to be only about 5% lower than that predicted for a sphere with homogeneous charge. Hence, the effect of lysozyme shape and charge heterogeneity is not predicted to be significant.

If the zeta potential is smaller than $RT/F = 25.7$ mV, the linearized Poisson–Boltzmann equation can be applied, yielding the following relation between ζ and the protein charge, Z_p :⁹¹

$$\frac{F\zeta}{RT} = Z_p \frac{\lambda_B}{R_p} \frac{1}{1 + \kappa R_p} \quad (23)$$

The value of Z_p in eq 23 corresponds to the particle charge at the shear interface. This interface is located slightly outside the

Stern layer. Thus, this charge value of Z_p should be very close to that of Z_p in eq 11.

The behavior of the electrophoretic mobility as described by eq 22 represents the contribution of the electrophoretic effect to diffusiophoresis. Another phenomenon specific to diffusiophoresis is represented by the chemiphoretic effect.^{33,89,94} This is related to the perturbation of the electrical double layer from its equilibrium structure causing a salt concentration gradient. Indeed, the double layer on the low C_2 side of a particle is slightly expanded compared to the double layer on the high C_2 side. This brings about a pressure gradient along the direction of ∇C_2 , which causes a particle to migrate from low to high salt concentration. As we shall see below, the chemiphoretic effect in the case of lysozyme is relatively small compared to the corresponding electrophoretic effect.

The electrophoretic effect is expected to dominate the behavior of lysozyme $\hat{D}_{12}(C_2)$ at low salt concentration. As in the case of u_p , $\hat{D}_{12}(C_2)$ will sharply decrease as the ionic strength increases. This nonlinear behavior qualitatively explains the very low value of Z_p obtained from a_{12} based on linear extrapolation. As the salt concentration increases, the contributions of protein hydration and preferential hydration described by N_w and \hat{D}_{12}^{-1} become relatively more important.

To take into account electrophoretic, chemiphoretic, and hydration effects in the behavior of lysozyme $\hat{D}_{12}(C_2)$, we modify eq 9a in the following way:

$$\hat{D}_{12} = \frac{|Z_p|}{2(1 + \kappa R_p)} \left[f_{\text{elec}}(\kappa R_p) \frac{D_- - D_+}{D_- + D_+} - \frac{1}{8} f_{\text{chem}}(\kappa R_p) \frac{F|\zeta|}{RT} \right] + b'_{12} C_2 \quad (24)$$

where $R_p = 1.864$ nm is the hydrodynamic radius of lysozyme calculated using the Stokes–Einstein equation (see Results). According to eq 24, the net value of $\hat{D}_{12}(C_2)$ is the sum of three terms. The first and second terms in the square brackets describe the electrophoretic and chemiphoretic effects, respectively. Note that the electrophoretic term is positive because $D_- > D_+$ for lysozyme in the presence of NaCl, while the chemiphoretic term is always negative independent of the difference in ion mobilities. The function

$$f_{\text{chem}}(x) = 1.5 - 0.5e^{2x} [10E_6(2x) + 7E_8(2x)] - 60e^{2x} E_7(x) [E_3(x) - E_5(x)] + 2e^x [3E_3(x) + 9E_4(x) - 7E_5(x) - 15E_{16}(x)]$$

was given by Huan and Wei,⁹⁴ and analytically describes the effect of double layer thickness on the chemiphoretic contribution. This effect was first described by Prieve and Roman, who previously published numerical results equivalent to the reported function.⁹⁵ The value of this function varies between $f_{\text{chem}}(0) = 0$ for a sphere at zero ionic strength to $f_{\text{chem}}(\infty) = 1.5$ for a planar surface. Note that eq 24 is consistent with eq 18 because they coincide in the limit of $C_2 = 0$. The third term is described by the slope b'_{12} and is related to protein–salt specific interactions. This parameter replaces b_{12} of eq 9a.

We apply the method of nonlinear least squares to our $\hat{D}_{12}(C_2)$ values in Figure 4. We obtain $Z_p = 7.4 \pm 0.5$ and $b'_{12}/\bar{V}_0 = 33 \pm 1$. This value of Z_p was then inserted into eq 23 to

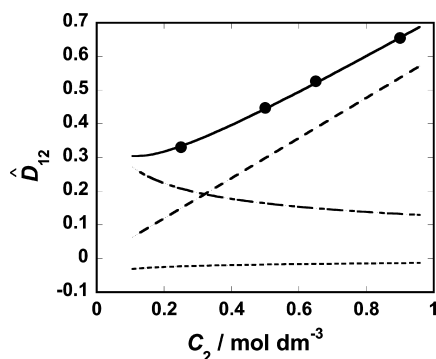


Figure 4. Normalized diffusiohoresis coefficient, \hat{D}_{12} , as a function of C_2 (solid circles). The solid curve describes the fit of the experimental results according to eq 24. The three terms in eq 24 characterizing the electrophoretic effect (---), the chemiphoretic effect (---), and protein–salt specific interactions (---) are also shown.

calculate ζ for our experimental salt concentrations to verify that $\zeta < 25.7$ mV (see Table 4).

Table 4. Calculated Values of Zeta Potential

$C_2/\text{mol dm}^{-3}$	κ^{-1}/nm	κR_p	ζ/mV
0.250	0.608	3.06	18
0.500	0.430	4.33	14
0.650	0.377	4.94	12
0.900	0.320	5.81	11

Figure 4 shows the behavior of $\hat{D}_{12}(C_2)$ obtained from our fit based on eq 24. Moreover, the three contributions to the expression of \hat{D}_{12} taken separately are also shown. We can see that the magnitude of the chemiphoretic term is small compared to that of the electrophoretic term at any salt concentration. We further observe that the electrophoretic term is dominant at low salt concentrations ($C_2 < 0.2$ mol dm⁻³), while the b'_{12} term prevails at high salt concentrations.

The value of Z_p extracted from eq 24 is now found to be in good agreement with that obtained from eq 11. The value of $b'_{12}/\bar{V}_0 = 33 \pm 1$ is slightly higher than $b_{12}/\bar{V}_0 = 29 \pm 1$. This small discrepancy has no effect on the interpretation of the slopes associated with eqs 11 and 17. Indeed, taking into account the electrophoretic effect seems critical for the examination of $\hat{D}_{12}(C_2)$ but not for that of $\lambda(C_2)$. Thus, we can still apply eqs 11 and 17 to eq 7a and write $b'_{12} \cong b_{12} = \bar{V}_0(N_w + \hat{D}_{12}^{-1})$ from the comparison with eq 9a. If we assume that protein hydration represents the dominant contribution to the value of \hat{D}_{12}^{-1} , we deduce that $b'_{12} \cong \bar{V}_0(N_w - n_w)$. We can interpret this result by considering that diffusiohoresis of protein molecules from high to low salt concentration is driven by protein preferential hydration (i.e., protein–salt repulsive interactions) as described by the excess of water, N_w . However, the effect of N_w on \hat{D}_{12} is reduced by the fact the n_w water molecules in the protein hydration shell remain attached to the macromolecule as diffusiohoresis occurs.

We can also use eq 24 to derive an expression for λ . Indeed, if we insert eq 24 into eq 7a, eq 17 can be rewritten in the following way:

$$\lambda = \frac{|Z_p|}{2} \left[\left(1 + \frac{f_{\text{elec}}(\kappa R_p)}{1 + \kappa R_p} \right) \tau_+ + \left(1 - \frac{f_{\text{elec}}(\kappa R_p)}{1 + \kappa R_p} \right) \tau_- + \frac{1}{8} \frac{f_{\text{chem}}(\kappa R_p) F |\zeta|}{1 + \kappa R_p RT} \right] + n_w \bar{V}_0 C_2 \quad (25)$$

We finally observe that the value of Z_p extracted from \hat{D}_{12} , together with the values of D_p in Table 2, can be utilized to estimate lysozyme electrophoretic mobility as a function of ionic strength according to eqs 22 and 23. Our estimated electrophoretic mobility can be then compared with literature data obtained from electrophoresis measurements. The experimental value of $u_p = 6.34 \times 10^{-9}$ m² s⁻¹ V⁻¹ was obtained from the classical electrophoresis experiments of Beychok and Warner at 0 °C, pH 4.5, and 0.15 M ionic strength.⁹⁶ This experimental work has been an important reference for several theoretical studies on protein electrophoresis.⁷⁹ If we insert $Z_p = 7.4$ and the lysozyme tracer-diffusion coefficient into eq 22, we estimate $u_p \approx 12 \times 10^{-9}$ m² s⁻¹ V⁻¹ at the ionic strength of 0.15 M and 25 °C. The chief effect of temperature on u_p can be taken into account by considering the corresponding effect on water viscosity. Since water viscosity increases by a factor of 2.01 when the temperature is decreased from 25 to 0 °C,⁷⁴ we calculate $u_p \approx 6 \times 10^{-9}$ m² s⁻¹ V⁻¹ at 0 °C. This estimate is in very good agreement with the experimental literature value.

SUMMARY AND CONCLUSIONS

We have measured the four ternary diffusion coefficients for the lysozyme–salt–water system as a function of protein and salt concentrations. We have introduced two normalized cross-diffusion coefficients, $\hat{D}_{12} \equiv \lim_{C_1 \rightarrow 0} [C_2 D_{12} / (2\gamma_s C_1 D_p)]$ and $\hat{D}_{21} \equiv \lim_{C_1 \rightarrow 0} (D_{21} / D_s)$, describing protein diffusiohoresis and salt osmotic diffusion respectively as a function of salt concentration. The coefficient \hat{D}_{21} is approximately a thermodynamic quantity, related to the thermodynamic parameter $\gamma \equiv -\lim_{C_1 \rightarrow 0} (\partial m_2 / \partial m_1)_{\mu_2, T, p'}$ while the coefficient \hat{D}_{12} is given by the difference between γ and the transport parameter $\lambda \equiv -\lim_{C_1 \rightarrow 0} (L_{12} / L_{11})$. The observed behavior of $\hat{D}_{21}(C_2)$ is related to common-ion and excluded-volume effects. The examination of γ as a function of C_2 has led to determination of the protein charge, Z_p , and the excess of water, N_w . These two parameters characterize water-mediated protein–salt thermodynamic interactions.

Values of \hat{D}_{12} and \hat{D}_{21} were utilized not only to extract $\lambda(C_2)$ but also \hat{D}_{12} , the normalized protein–salt S–M diffusion coefficient. We find that that \hat{D}_{12} is negative. This implies that it is unphysical to describe solute–solvent S–M diffusion coefficients as friction coefficients. Our finding was explained by considering the effect of protein hydration.

In relation to protein diffusiohoresis, we find that even minor inaccuracies in the estimates of S–M diffusion coefficients and values of preferential-interaction coefficients can lead to large errors in the estimated value of \hat{D}_{12} . The electrophoretic effect dominates the behavior of \hat{D}_{12} at low salt concentrations, while the contribution of protein–salt specific interactions, described by \hat{D}_{12} and N_w , prevail at high salt concentrations. Our \hat{D}_{12} results were also employed to accurately estimate the value of lysozyme electrophoretic mobility.

This work represents the first accurate experimental investigation reporting protein diffusiophoresis in aqueous salt solution and a protein–salt S – M diffusion coefficient. It will provide guidance for understanding and modeling the effect of concentration gradients in protein–salt aqueous systems relevant to diffusion-based mass-transfer technologies and transport in living systems.

■ ASSOCIATED CONTENT

● Supporting Information

Table of volume-fixed diffusion coefficients and partial molar volumes. Derivation of the expression of λ from the Stefan–Maxwell equations. Derivation of $\hat{D}_{12}^{-1} = -n_w$ based on protein hydration. This material is available free of charge via the Internet at <http://pubs.acs.org>.

■ AUTHOR INFORMATION

Corresponding Author

*Tel.: (817) 257-6215. Fax: (817) 257-5851. E-mail: O. Annunziata@tcu.edu.

Present Address

†Department of Physics, “Politehnica” University, Bucharest, 76990, Romania.

Notes

The authors declare no competing financial interest.

■ ACKNOWLEDGMENTS

This paper is dedicated to the memory of our colleague and friend Donald G. Miller, who has provided invaluable contributions to the fields of multicomponent diffusion and electrolyte solutions. We thank Manfred E. Zeidler for technical assistance with the Gosting diffusimeter. This research was supported by the ACS Petroleum Research Fund (47244-G4), the NASA BioTechnology Program (NAG8-1356), and TCU RCAF funds.

■ REFERENCES

- (1) Bird, R. B. *AIChE J.* **2003**, *50*, 273–287.
- (2) Cussler, E. L. *Diffusion: Mass Transfer in Fluid Systems*; Cambridge University Press: Cambridge, U.K., 1997.
- (3) Curtiss, C. F.; Bird, R. B. *Ind. Eng. Chem. Res.* **1999**, *38*, 2515–2522.
- (4) Tyrrell, H. J. V.; Harris, K. R. *Diffusion in Liquids*; Butterworths: London, 1984.
- (5) Wesselingh, J. A. *J. Controlled Release* **1993**, *24*, 47–60.
- (6) Higuchi, T. *J. Pharm. Sci.* **1961**, *50*, 874–875.
- (7) Keurentjes, J. T. F.; Janssen, A. E. M.; Broeka, A. P.; Van der Padta, A.; Wesselingh, J. A.; Van’T Riet, K. *Chem. Eng. Sci.* **1992**, *47*, 1963–1971.
- (8) Petsev, D. N.; Chen, K.; Gliko, O.; Vekilov, P. G. *Proc. Natl. Acad. Sci. U.S.A.* **2003**, *100*, 792–796.
- (9) Garcia-Ruiz, J. M. *Methods Enzymol.* **2003**, *368*, 130–154.
- (10) Postma, M.; Van Haastert, P. J. *Biophys. J.* **2001**, *81*, 1314–1323.
- (11) Thorne, R. G.; Lakkaraju, A.; Rodriguez-Boulan, E.; Nicholson, C. *Proc. Natl. Acad. Sci. U.S.A.* **2008**, *105*, 8416–8421.
- (12) Sochacki, K. A.; Shkel, I. A.; Record, M. T.; Weisshaar, J. C. *Biophys. J.* **2011**, *100*, 22–31.
- (13) Miguez, D. G.; Vanag, V. K.; Epstein, I. R. *Proc. Natl. Acad. Sci. U.S.A.* **2007**, *104*, 6992–6997.
- (14) Park, S.; Agmon, N. *J. Phys. Chem. B* **2008**, *112*, 12104–12114.
- (15) Vanag, V. K.; Epstein, I. R. *Chaos* **2005**, *15*, 047510.
- (16) Allshouse, M. R.; Barad, M. F.; Peacock, T. *Nat. Phys.* **2010**, *6*, 516–519.
- (17) Page, M. A. *Nat. Phys.* **2010**, *6*, 486–487.
- (18) Kanjickal, D. G.; Lopina, S. T. *Crit. Rev. Ther. Drug Carrier Syst.* **2004**, *21*, 345–386.
- (19) Whitesides, G. M. *Nature* **2006**, *442*, 368–373.
- (20) Abécassis, B.; Cottin-Bizonne, C.; Ybert, C.; Ajdari, A.; Bocquet, L. *Nat. Mater.* **2008**, *7*, 785–789.
- (21) Weigl, B. H.; Yager, P. *Science* **1999**, *283*, 346–347.
- (22) Atencia, J.; Beebe, D. J. *Nature* **2005**, *437*, 648–655.
- (23) Jervais, T.; Jensen, K. F. *Chem. Eng. Sci.* **2006**, *61*, 1102–1121.
- (24) Gosting, L. J. *Adv. Protein Chem.* **1956**, *11*, 429–554.
- (25) Albright, J. G.; Annunziata, O.; Miller, D. G.; Paduano, L.; Pearlstein, A. J. *J. Am. Chem. Soc.* **1999**, *121*, 3256–3266.
- (26) Leaist, D. G. *J. Phys. Chem.* **1989**, *93*, 474–479.
- (27) Vergara, A.; Capuano, F.; Paduano, L.; Sartorio, R. *Macromolecules* **2006**, *39*, 4500–4506.
- (28) Vanag, V. K.; Epstein, I. R. *Phys. Chem. Chem. Phys.* **2009**, *11*, 897–912.
- (29) Liu, X.; Bardow, A.; Vlugt, T. J. H. *Ind. Eng. Chem. Res.* **2011**, *50*, 4776–4782.
- (30) Price, P. E.; Romdhane, I. H. *AIChE J.* **2003**, *49*, 309–322.
- (31) Schaeiwitz, J. A.; Lechnick, W. J. *Chem. Eng. Sci.* **1984**, *39*, 799–807.
- (32) Wall, S. *Curr. Opin. Colloid Interface Sci.* **2010**, *15*, 119–124.
- (33) Anderson, J. L. *Ann. Rev. Fluid Mech.* **1989**, *21*, 61–99.
- (34) Abécassis, B.; Cottin-Bizonne, C.; Ybert, C.; Ajdari, A.; Bocquet, L. *New J. Phys.* **2009**, *11*, 075022.
- (35) Lightfoot, E. N.; Cussler, E. L.; Rettig, R. L. *AIChE J.* **1962**, *8*, 708–709.
- (36) Wesselingh, J. A.; Krishna, R. *Mass Transfer in Multicomponent Mixtures*; VSSD: Delft, The Netherlands, 2006.
- (37) Zhang, Y.; Cremer, P. S. *Curr. Opin. Chem. Biol.* **2006**, *10*, 658–663.
- (38) Auton, M.; Bolen, D. W. *Proc. Natl. Acad. Sci. U.S.A.* **2005**, *102*, 15065–15068.
- (39) Timasheff, S. N. *Proc. Natl. Acad. Sci. U.S.A.* **2002**, *99*, 9721–9726.
- (40) Ru, M. T.; Hirokane, S. Y.; Lo, A. S.; Dordick, J. S.; Reimer, J. A.; Clark, D. S. *J. Am. Chem. Soc.* **2000**, *122*, 1565–1571.
- (41) Vekilov, P. G. *Cryst. Growth Des.* **2007**, *7*, 2239–2246.
- (42) Liu, W.; Cellmer, T.; Keerl, D.; Prausnitz, J. M.; Blanch, H. W. *Biotechnol. Bioeng.* **2005**, *90*, 482–490.
- (43) Fine, B. M.; Lomakin, A.; Ogun, O. O.; Benedek, G. B. *J. Chem. Phys.* **1995**, *104*, 326–335.
- (44) Schmitz, K. S. *Introduction to Dynamic Light Scattering by Macromolecules*; Academic Press: San Diego, CA, USA, 1990.
- (45) Annunziata, O.; Buzatu, D.; Albright, J. G. *Langmuir* **2005**, *21*, 12085–12089.
- (46) Sutherland, E.; Mercer, S. M.; Everist, M.; Leaist, D. G. *J. Chem. Eng. Data* **2009**, *54*, 272–278.
- (47) Einstein, A. *Ann. Phys.* **1905**, *17*, 549–560.
- (48) Tanford, C. *Physical Chemistry of Macromolecules*; Wiley: New York, 1961; p 356.
- (49) Lomakin, A.; Teplow, D. B.; Benedek, G. B. *Quasielastic Light Scattering for Protein Assembly Studies*. In *Methods in Molecular Biology Amyloid Proteins, Vol. 299: Methods and Protocols*; Sigurdsson, E. M., Ed.; Humana Press: Totowa, NJ, USA, 2005; pp 153–174.
- (50) Toor, H. L. *AIChE J.* **1957**, *3*, 198–207.
- (51) Annunziata, O.; Paduano, L.; Pearlstein, A. J.; Miller, D. G.; Albright, J. G. *J. Am. Chem. Soc.* **2000**, *122*, 5916–5928.
- (52) Annunziata, O.; Paduano, L.; Albright, J. G. *J. Phys. Chem. B* **2006**, *110*, 16139–16147.
- (53) Annunziata, O.; Paduano, L.; Pearlstein, A. J.; Miller, D. G.; Albright, J. G. *J. Phys. Chem. B* **2006**, *110*, 1405–1415.
- (54) Annunziata, O.; Paduano, L.; Albright, J. G. *J. Phys. Chem. B* **2007**, *111*, 10591–10598.
- (55) Annunziata, O.; Payne, A.; Wang, Y. *J. Am. Chem. Soc.* **2008**, *130*, 13347–13352.
- (56) Arakawa, T.; Timasheff, S. N. *Biochemistry* **1982**, *21*, 6545–6552.
- (57) Record, M. T.; Anderson, C. F. *Biophys. J.* **1995**, *68*, 786–794.

- (58) Annunziata, O.; Buzatu, D.; Albright, J. G. *J. Chem. Eng. Data* **2011**, *56*, 4849–4852.
- (59) Miller, D. G.; Vitagliano, V.; Sartorio, R. *J. Phys. Chem.* **1986**, *90*, 1509–1519.
- (60) Woolf, L. A.; Miller, D. G.; Gosting, L. J. *J. Am. Chem. Soc.* **1962**, *84*, 317–331.
- (61) Miller, D. G. *J. Phys. Chem.* **1959**, *63*, 570–578.
- (62) Zhang, H.; Annunziata, O. *Phys. Chem. Chem. Phys.* **2009**, *11*, 8923–8932.
- (63) Miller, D. G. The Onsager Relations; Experimental Evidence. In *Foundations of Continuum Thermodynamics*; Delgado Domingos, J. J., Nina, M. N. R., Whitelaw, J. H., Eds.; MacMillan Press: London, 1974; pp 185–214.
- (64) Onsager, L. *Phys. Rev.* **1931**, *37*, 405–426.
- (65) The diffusio-phoretic mobility of a particle has been defined as the $(\nabla \ln C_2)/(J_1/C_1)$ ratio (see eq 2 in ref 20, for example), where $\nabla \ln C_2$ is the driving force and J_1/C_1 is the particle migration velocity. Here, since the salt concentration can be arbitrarily large, we have replaced $\nabla \ln C_2$ with $\nabla \mu_2/RT$, which also takes into account thermodynamic nonideality.
- (66) We use the subscript “1” for the protein, the subscript “2” for the salt, and the subscript “0” for the solvent consistent with the literature on multicomponent diffusion. However, the subscript “2” for the protein, the subscript “3” for the salt, and the subscript “1” for the solvent are extensively used in relation to the thermodynamic description of protein mixtures.
- (67) Courtneay, E. S.; Capp, M. W.; Anderson, C. F.; Record, M. T. *Biochemistry* **2000**, *39*, 4455–4471.
- (68) Dunlop, P. J.; Gosting, L. J. *J. Phys. Chem.* **1959**, *63*, 86–93.
- (69) Miller, D. G.; Albright, J. G. Optical Methods. In *Measurement of the Transport Properties of Fluids: Experimental Thermodynamics*; Wakeham, W. A., Nagashima, A., Sengers, J. V., Eds.; Blackwell Scientific Publications: Oxford, U.K., 1991; Vol. III, pp 272–294.
- (70) Miller, D. G. *J. Phys. Chem.* **1988**, *92*, 4222–4226.
- (71) Rad, J. A.; Miller, D. G. *J. Solution Chem.* **1979**, *8*, 701–716.
- (72) Miller, D. G. *J. Phys. Chem.* **1966**, *70*, 2639–2659.
- (73) Zhang, H.-L.; Han, S.-J. *J. Chem. Eng. Data* **1996**, *41*, 516–520.
- (74) Kestin, J.; Sokolov, M.; Wakeham, W. A. *J. Phys. Chem. Ref. Data* **1978**, *7*, 941–948.
- (75) Parsegian, V. A.; Rand, R. P.; Rau, D. C. *Proc. Natl. Acad. Sci. U.S.A.* **2000**, *97*, 3987–3992.
- (76) Tanford, C.; Roxby, R. *Biochemistry* **1972**, *11*, 2192–2198.
- (77) Girard, E.; Chantalat, L.; Vicat, J.; Kahn, R. *Acta Crystallogr., Sect. D* **2002**, *58*, 1–9.
- (78) Lim, K.; Nadarajah, A.; Forsythe, E. L.; Pusey, M. L. *Acta Crystallogr., Sect. D* **1998**, *54*, 899–904.
- (79) Allison, S. A.; Potter, M.; McCammon, J. A. *Biophys. J.* **1995**, *68*, 2261–2270.
- (80) The partial molar volume, \bar{V}_1 , describes the increment in solution volume associated with the infinitesimal addition of lysozyme chloride. This addition will also produce a change in the molar volume of water surrounding protein molecules. If the number of perturbed water molecules is N_w , we can deduce that $\bar{V}_1 = V_p + N_w(\bar{V}_w - \bar{V}_0)$. This is the same as $\bar{V}_1 + N_w\bar{V}_0 = V_p + N_wV_w$. We also observe that ≈ 8 free chloride ions also contribute to \bar{V}_1 . By using the partial-molar-volume data of KCl in ref 53 and assuming that the partial molar volume of chloride ions is the same as that of potassium ions, we can estimate that each chloride ion contributes $\approx 0.015 \text{ dm}^3 \text{ mol}^{-1}$ to the value of \bar{V}_1 . This implies that $\approx 0.12 \text{ dm}^3 \text{ mol}^{-1}$ of $\bar{V}_1 = 10.2 \text{ dm}^3 \text{ mol}^{-1}$ represents the contribution (1.2%) of the free chloride ions.
- (81) Bearman, R. J. *J. Phys. Chem.* **1961**, *65*, 1961–1968.
- (82) Krishna, R. *Chem. Eng. J.* **1987**, *35*, 19–24.
- (83) Albright, J. G. *J. Phys. Chem.* **1969**, *73*, 1280–1286.
- (84) Robinson, R. A.; Stokes, R. H. *Electrolyte Solutions*; Dover: Mineola, NY, Englewood Cliffs, NJ, USA, 2002.
- (85) Newman, J. S. *Electrochemical Systems*, 2nd ed.; Prentice-Hall: Englewood Cliffs, NJ, USA, 1991.
- (86) Wesselingh, J. A.; Krishna, R. *Mass Transfer in Multicomponent Mixtures*; VSSD: Delft, The Netherlands, 2006.
- (87) Harris, K.; Woolf, L. E. *J. Chem. Soc., Faraday Trans. 1* **1980**, *76*, 377–385.
- (88) Annunziata, O. *J. Phys. Chem. B* **2008**, *112*, 11968–11975.
- (89) Timasheff, S. N. *Biochemistry* **2002**, *41*, 13473–13482.
- (90) Prieve, D. C. *Adv. Colloid Interface Sci.* **1982**, *16*, 321–335.
- (91) Carbeck, J. D.; Negin, R. S. *J. Am. Chem. Soc.* **2001**, *123*, 1252–1253.
- (92) Henry, D. C. *Proc. R. Soc. London, A* **1931**, *133*, 106–129.
- (93) Russel, W. B.; Saville, D. A.; Schowalter, W. R. *Colloidal Dispersions*; Cambridge University Press: New York, 1989.
- (94) Huan, J. K.; Wei, Y. K. *Langmuir* **2000**, *16*, 5289–5294.
- (95) Prieve, D. C.; Roman, R. *J. Chem. Soc., Faraday Trans. 2* **1987**, *83*, 1287–1306.
- (96) Beychok, S.; Warner, R. C. *J. Am. Chem. Soc.* **1959**, *81*, 1892–1897.